Jeje *et al. Beni-Suef Univ J Basic Appl Sci* (2024) 13:16
https://doi.org/10.1186/s43088-024-00474-0

Beni-Suef University Journal of Basic and Applied Sciences

RESEARCH

Open Access

Impact behavior of spark plasma sintered Ti–Al–Mo/TiN composites: a finite element analysis approach using Abaqus CAE

Samson Olaitan Jeje[1*], Tawanda Marazani[1] and Mxolisi Brendon Shongwe[1]

Abstract

Background The utilization of Finite Element Analysis (FEA) has emerged as a crucial methodology in the field of structural and elasticity analysis, facilitating researchers in their understanding of material responses to diverse thermal or structural loads. This study investigates the utilization of FEA to simulate the Impact characteristics of titanium composites, with specific emphasis on the Charpy impact test. The research utilizes the Abaqus Explicit software, which is widely recognized for its explicit dynamic analysis functionalities, to simulate high-speed and short-duration events such as impacts. The primary objective of this study is to examine the impact behavior of Ti–7Al–1mo/TiN composites fabricated through the spark plasma sintering technique. The impact behavior is simulated using FEA, wherein the shear failure model is utilized to replicate fracture phenomena. This paper examines the methodology employed in the FEA approach, with a particular focus on various factors including boundary conditions, explicit dynamic analysis settings, and material properties.

Results The outcomes and analyses involve the examination of the von Mises stress distribution, displacement magnitude, and energy behavior of the models that were tested. Reinforcement of Ti–Al–Mo ternary alloy with TiN led to a progressive increase in maximum von Mises stress, reaching a peak at 3 wt% TiN. Conversely, displacement magnitude decreased with increasing TiN content, with CP-Ti and the unreinforced alloy exhibiting the highest values. Absorbed energy also declined with higher TiN levels. While models containing 5 and 7 wt% TiN displayed limited plastic deformation before fracture, composites with ≤ 3 wt% TiN maintained acceptable ductility despite enhanced strength and stiffness.

Conclusion The FEA methodology effectively simulates the Charpy impact characteristics of Ti–7Al–1Mo/TiN composites, thereby offering significant contributions to understanding their mechanical behaviors. These findings suggest that TiN reinforcement up to 3 wt% presents a promising strategy for improving the mechanical performance of Ti–Al–Mo alloys while minimizing the trade-off in toughness. This research emphasizes the inherent trade-off between toughness and strength/stiffness, suggesting the possibility of optimizing the composition of materials to suit particular applications. This study makes a valuable contribution to the expanding field of impact behavior research, demonstrating the potential of FEA, specifically utilizing Abaqus Explicit software, for enhancing material design and evaluation.

Keywords Titanium matrix composite, Finite element analysis, Abaqus Explicit software, Charpy impact

*Correspondence:
Samson Olaitan Jeje
jejesamsonn@gmail.com
Full list of author information is available at the end of the article

1 Background

Titanium composites have emerged as crucial materials in contemporary engineering applications across various industries, including aerospace, automotive, and sports, due to their notable strength-to-weight ratio and exceptional resistance to corrosion [1–3]. Reinforcing titanium (Ti) and its alloy with ceramics such as titanium nitride (TiN), alumina (Al_2O_3), zirconia (ZrO_2), silicon carbide (SiC), titanium diboride (TiB_2), titanium carbide (TiC), titanium carbonitride (TiCN), and silicon nitride (Si3N4) has received excellent evaluations [2]. The focus on transition-metal nitride (TiN) arises from its exceptional characteristics. These qualities include elevated hardness, superior fracture toughness, exceptional thermal and chemical stability, as well as resistance to oxidation and corrosion [4, 5].The comprehension of the impact behavior of these materials is of utmost importance in guaranteeing the safety and dependability of structures, particularly as they are being employed more frequently in high-stress settings [6]. Traditional experimental methods, although possessing inherent value, frequently entail significant time and financial investments. The utilization of computational simulations, specifically finite element analysis (FEA), has significantly transformed the examination of material response to dynamic loading circumstances [7]. This work delves into the evolution of computational modeling with a focus on the impact behavior of titanium composite, emphasizing the utilization of Abaqus Explicit software, a powerful tool for analysis that involves explicit dynamics.

Researchers use FEA methods and theories to address the imperative need for resolving simple and intricate structural and elasticity analyses. FEA is utilized in conjunction with traditional testing methods to analyze the behavior of materials and predict their response to structural or thermal loads. To accurately anticipate the stresses and strains resulting from external forces that induce deformations, a comprehensive understanding of the intricate geometry and mechanical properties of the samples under examination is imperative. Zienkiewiez and Cheung [8] made scholarly contributions that can be attributed to the origins of the first published book in the field of FEA.

In previous years, there have been research efforts dedicated to the advancement and understanding of the fracture behavior of materials; particularly in response to sudden shocks and impacts. The study conducted by Lammari et al. [9] focuses on validating components that are subjected to sudden impacts in mechanical systems. It highlights the significance of taking into account various factors in the intricate Charpy impact test. The numerical models of the Charpy test, guided by the Johnson–Cook model, provided valuable insights into material reactions to sudden mechanical stresses. The conclusion highlighted the significance of notch geometry, revealing that the U-shaped notch demonstrated a higher safety factor during manufacturing than the V-shape, offering a practical implication for minimizing the risk of brittle fracture. Yu et al. [10] presented a nonlinear FEA framework, specifically addressing the impact energy required to fracture unnotched Charpy specimens using the Bulk Fracture Charpy Machine (BFCM). The comparison of different fracture initiation criteria showcased the versatility of the FEA methodology. The established benchmark between test and analysis allowed for the application of the stress triaxiality-dependent fracture criterion to various impacting scenarios, suggesting broader applicability in impact loading studies.

Extending the exploration into impact loading, Jeong et al. [11] conducted a nonlinear FEA study focusing on the energy required to fracture unnotched Charpy specimens under pendulum impact loading. The study incorporated an oversized pendulum impactor, the BFCM, and investigated various tank car steels. The inclusion of different material failure criteria, particularly the Bao-Wierzbicki criterion, demonstrated accurate reproduction of experimental data, showcasing the robustness of the elastic–plastic FEA framework. Madhusudhan et al. [12] study emphasizes the modeling and simulation of Charpy impact tests using ABAQUS, specifically targeting the evaluation of fracture energy in armor maraging steel 300. The variation in absorbed energy at different pendulum velocities and stress distribution at the V-notch provided a comprehensive understanding of material behavior under impact loading.

These studies contribute to the evolving landscape of fracture mechanics, combining experimental testing with advanced numerical simulations to unravel the complexities of material responses to sudden shocks. The integration of different methodologies not only refines our understanding of fracture properties but also opens avenues for broader applications in impact-loading scenarios across diverse materials and industries.

FEA, as a computer-aided engineering (CAE) tool, possesses attributes that are both user-friendly and yield effective outcomes, rendering it a prominent resource for researchers. Modeling impact behavior presents unique challenges due to the sudden, high-intensity loads involved. Achieving accurate results requires the consideration of numerous factors, such as material properties, boundary conditions, and loading conditions. The simulation of titanium composites gets complex due to their intricate microstructure and anisotropic properties [13].

Abaqus software, developed by Dassault Systèmes, has established itself as a leading choice for explicit dynamic analysis. The capability to effectively

manage high-velocity and short-duration events, such as impacts, has rendered it indispensable in investigating the response of materials under extreme conditions. The advanced algorithm in Abaqus Explicit greatly improves the accuracy of impact simulations by effectively managing large deformations, contact interactions, and materials failure [14]. The software's intuitive interface, combined with its powerful computational capabilities, has enabled researchers to explore the impact behavior of materials in greater depth.

The aerospace and automotive industries are at the forefront of employing titanium composites, capitalizing on their remarkable strength and lightweight characteristics. The utilization of Abaqus Explicit in computational role in the design of impact-resistance components for aircraft and automobiles. These simulations allow engineers to optimize the material composition and structural configurations, guaranteeing the safety of passengers and crew during unexpected events. The advancement of computational modeling and Abacus Explicit software has introduced a new era in the examination of the impact behavior, specifically in titanium composites. Researchers now have advanced tools to examine and enhance materials and structural designs, guaranteeing durability and security in various applications. Our previous work [2] experimentally investigated the density, microstructural evolution, and mechanical properties of Ti–7Al–1Mo/TiN. The composite was fabricated by employing the spark plasma sintering technique based on different weight percentages of TiN nanoceramic (0, 1, 3, 5, 7 wt%). This work further explores the impact behavior of Ti–7Al–1Mo/TiN using the FEA approach. This analysis was employed as a predictive tool to derive the quantitative measurement of the absorbed impact energy of the tested sample, thus offering insights into the material's toughness [15, 16]. This study sets the stage for highlighting the methodologies, and potentials of employing Abaqus Explicit software in the computational modeling of impact behavior in titanium composites.

2 Methods

The fabrication of the Ti–7Al–1Mo/TiN composite was accomplished through the utilization of the HHPD-25 FCT model spark plasma sintering machine, as detailed by Jeje et al. [2]. FEA was employed to simulate the impact behavior of the composites, utilizing the Abaqus Explicit software. The sample's dimensions (Fig. 1) were determined according to the ASTM E23 standard, while the Charpy impact behavior was simulated using a shear failure model. The corresponding plastic strain at element integration locations serves as the basis for the shear failure model, which assumes failure to occur when the damage parameter rises above 1. Equation 1 gives the damage parameter, ω [17].

$$\omega = \frac{\overline{\epsilon}_0^{pl} + \sum \Delta \overline{\epsilon}^{pl}}{\overline{\epsilon}_f^{pl}} \tag{1}$$

where $\overline{\epsilon}_f^{pl}$ is the strain at failure, $\overline{\epsilon}^{pl}$ is an increment of the equivalent plastic strain, and $\overline{\epsilon}_0^{pl}$ is any initial value of the equivalent plastic strain. The summing is carried out across all of the analysis's increments.

It is anticipated that the plastic strain rate, $\overline{\epsilon}^{pl}$; temperature; preset field variables; and a dimensionless pressure-deviatoric stress ratio, p/q (where p is the pressure stress and q is the Mises stress) will all affect the strain at failure, $\overline{\epsilon}_f^{pl}$. The strain at failure, $\overline{\epsilon}_f^{pl}$, can be defined in two ways. One way is to use direct tabular data, which provides a tabular representation of the dependencies. The strain at failure, denoted as $\overline{\epsilon}_f^{pl}$, is required to be represented as a tabular function in the creation of the shear failure model using direct tabular data. This tabular function should consider the equivalent plastic strain rate, the pressure-deviatoric stress ratio, temperature, and preset field variables.

Figure 2 depicts the finite element model configuration employed within the Abaqus Explicit software.

The simulation utilized the S.I. units as presented in Table 1. The 40 mm span length was utilized in

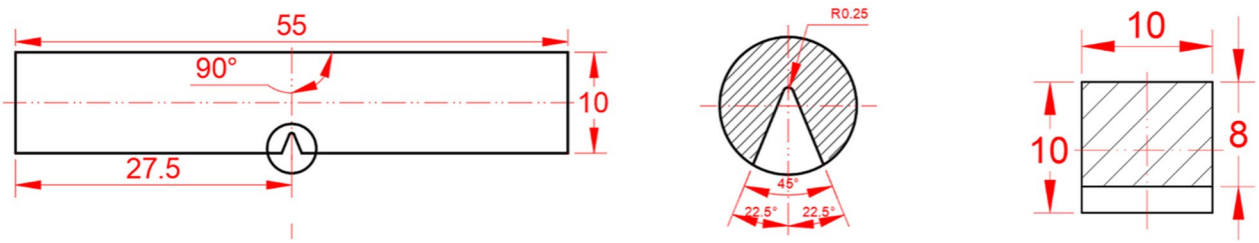

Fig. 1 A standard Charpy impact test specimen (Dimensions in mm) [18]

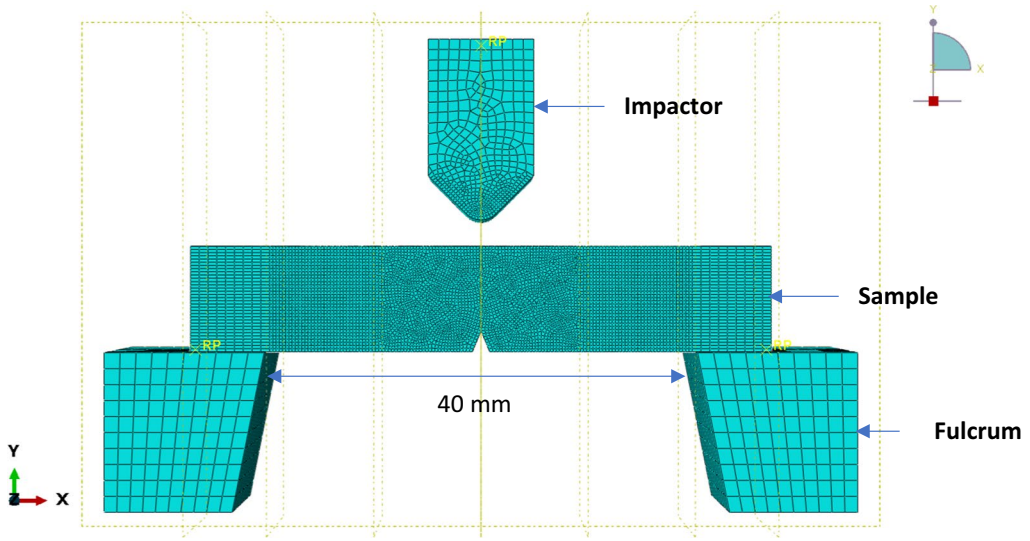

Fig. 2 The setup of the FEA model for the Charpy impact test

Table 1 Simulation quantity, along with its corresponding units within the International System of Units

Quantity	SI unit
Length	Meter (m)
Mass	Kilogram (kg)
Force	Newton (N)
Time	Second (s)
Stress	Pascal (Pa)
Energy	Joule (J)
Density	kg/m^3

accordance with the Charpy standard. The impactor was simulated as a rigid body with a mass of 3.367 kg, while the sample was assumed to be both homogeneous and deformable. The step type was dynamically assigned with explicit timing of 0.003 s. The partitioning of the sample was conducted by employing datum planes at distances of 7.5 mm and 40 mm. This approach aimed to establish a more distinct interaction surface between the sample and the impactor, as depicted in Fig. 3.

The interaction between the impactor and the sample is characterized by surface-to-surface contact, specifically

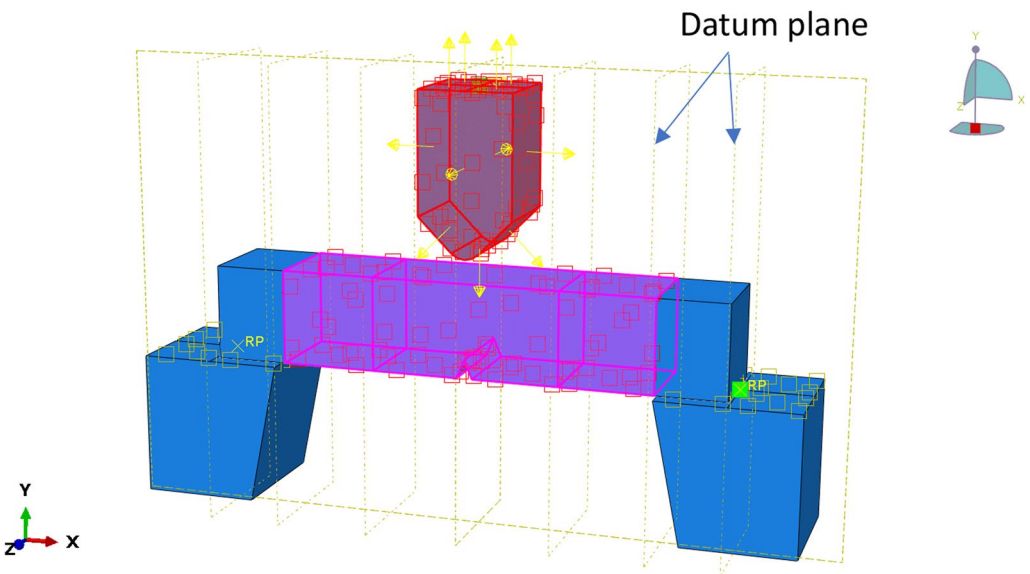

Fig. 3 Datum planes and interaction between the sample and impactor

employing a kinematic contact method for mechanical constraint formulation. The contact interaction property is defined as tangential behavior, utilizing a penalty friction formulation with a coefficient of friction determined from the experimental wear results of the samples. The model, consisting of the impactor and the sample, was discretized using an explicit element library. Hexagonal elements were employed, with the inclusion of hourglass element control and the activation of element deletion. The sample model consisted of a total of 192,576 nodes and 180,642 elements.

Three boundary conditions were established. Initially, it should be noted that the degree of freedom possessed by the impactor is limited to movement in the direction toward or away from the test sample. Specifically, the displacements U1, U3, UR1, UR2, and UR3 are equal, whereas U2 is not equal to zero. Here, the subscripts 1, 2, and 3 correspond to the *x*, *y*, and *z* directions, respectively. Furthermore, it should be noted that the fulcrum degree of freedom restricts movement in all directions, as indicated by the conditions U1 = U2 = U3 = UR1 = UR2 = UR3 = 0. Lastly, Fig. 4 illustrates that the initial velocity of the impactor was uniformly translational, with a magnitude of 5 m/s.

3 Results

3.1 Von Mises stress distribution of tested samples

Figure 5 illustrates the distribution of von Mises stress in the samples. The maximum stress value of CP-Ti (Fig. 5a) was determined to be 743.7 MPa, whereas in the Ti–7Al–1Mo ternary alloy, this value increased to 985 MPa. Furthermore, it was observed that the maximum stress exhibited an upward trend with an increase in the weight percentage of TiN nanoceramic in the simulated composites. Among these composites, Ti–7Al–1Mo/7TiN demonstrated the highest maximum stress value, reaching 1373 MPa.

Crack initiation was observed at the V-notch of all the tested samples. However, except for Ti–7Al–1Mo reinforced with 5 wt% and 7 wt% of TiN nanoceramic, all samples exhibited a certain degree of plastic deformation without crack propagation within the material. The Ti–7Al–1Mo alloy, when reinforced with 5 wt% and 7 wt% of TiN nanoceramic, exhibited observable shear banding phenomena.

3.2 Displacement magnitude of tested samples

Figure 6 illustrates the distribution of displacement magnitude within the models that were subjected to testing. The maximum displacement magnitude of CP-Ti is observed to be 4.003 mm before fracture occurs. However, there was a significant reduction of about 1.392 mm in the displacement magnitude of the Ti–7Al–1Mo ternary alloy. There is a further enhancement in the displacement magnitude of the TiN-reinforced composite, with the lowest recorded value being 1.934 mm for Ti–7Al–1Mo/3TiN. However, there are exceptions for composites containing 5 wt% and 7 wt% of TiN. They experienced the highest magnitude of maximum displacement of 4.241 mm and 4.801 mm respectively.

3.3 Energy behavior of the model of tested samples

Figure 7a, b depicts the kinetic energy of the impactor and the internal energy of the tested models, respectively. The experimental findings indicate that the amount of

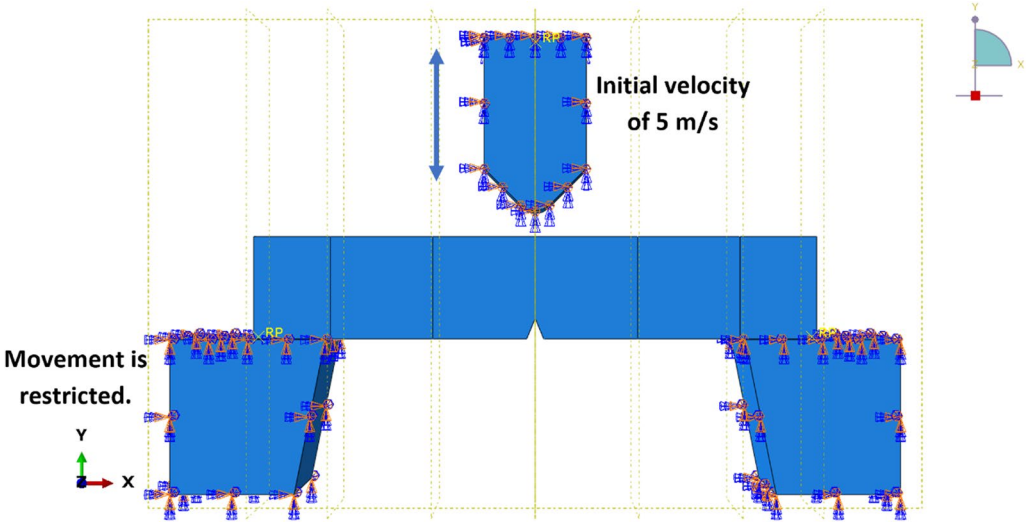

Fig. 4 Boundary conditions set for the model

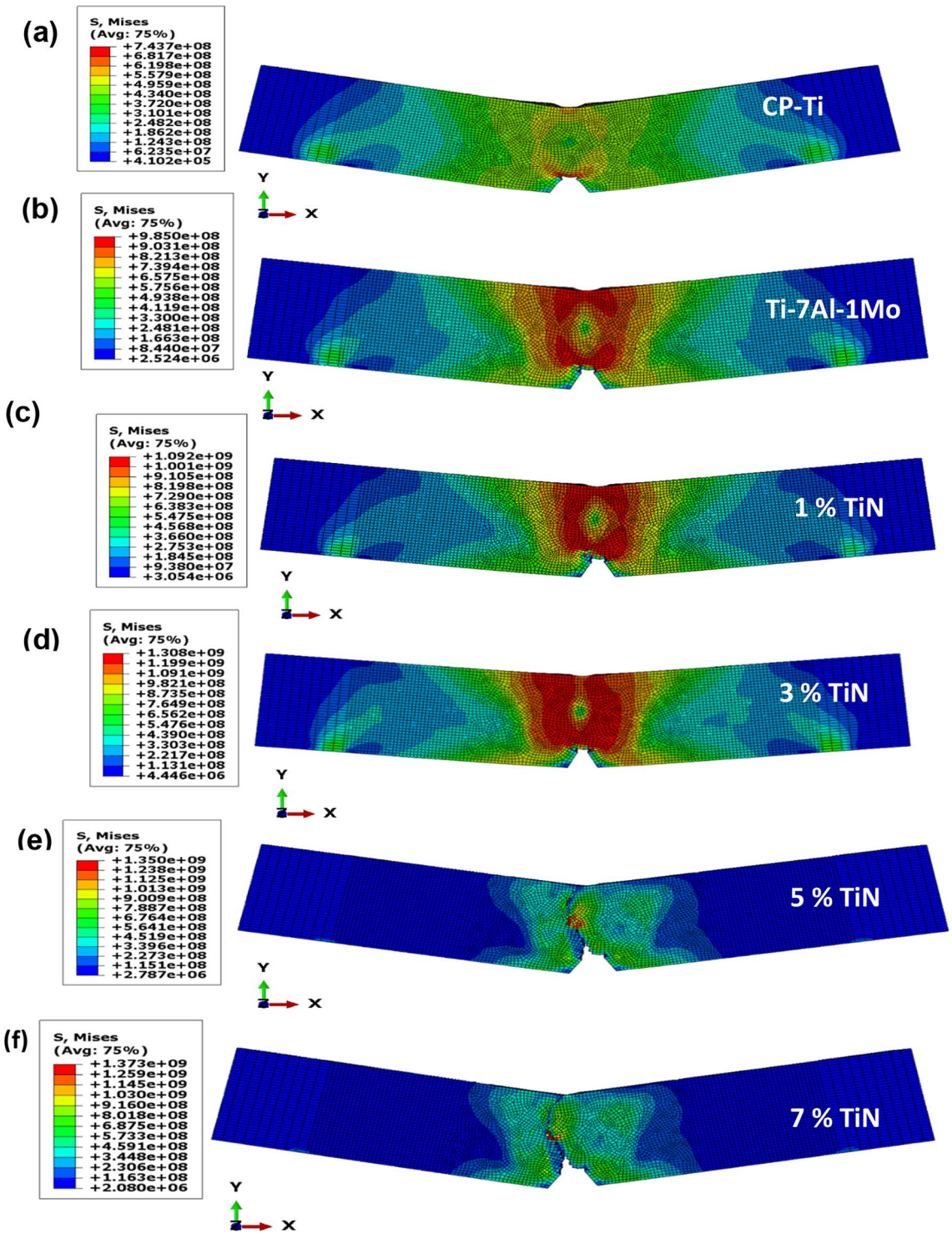

Fig. 5 Von Mises stress distribution of tested models with varying wt% of TiN

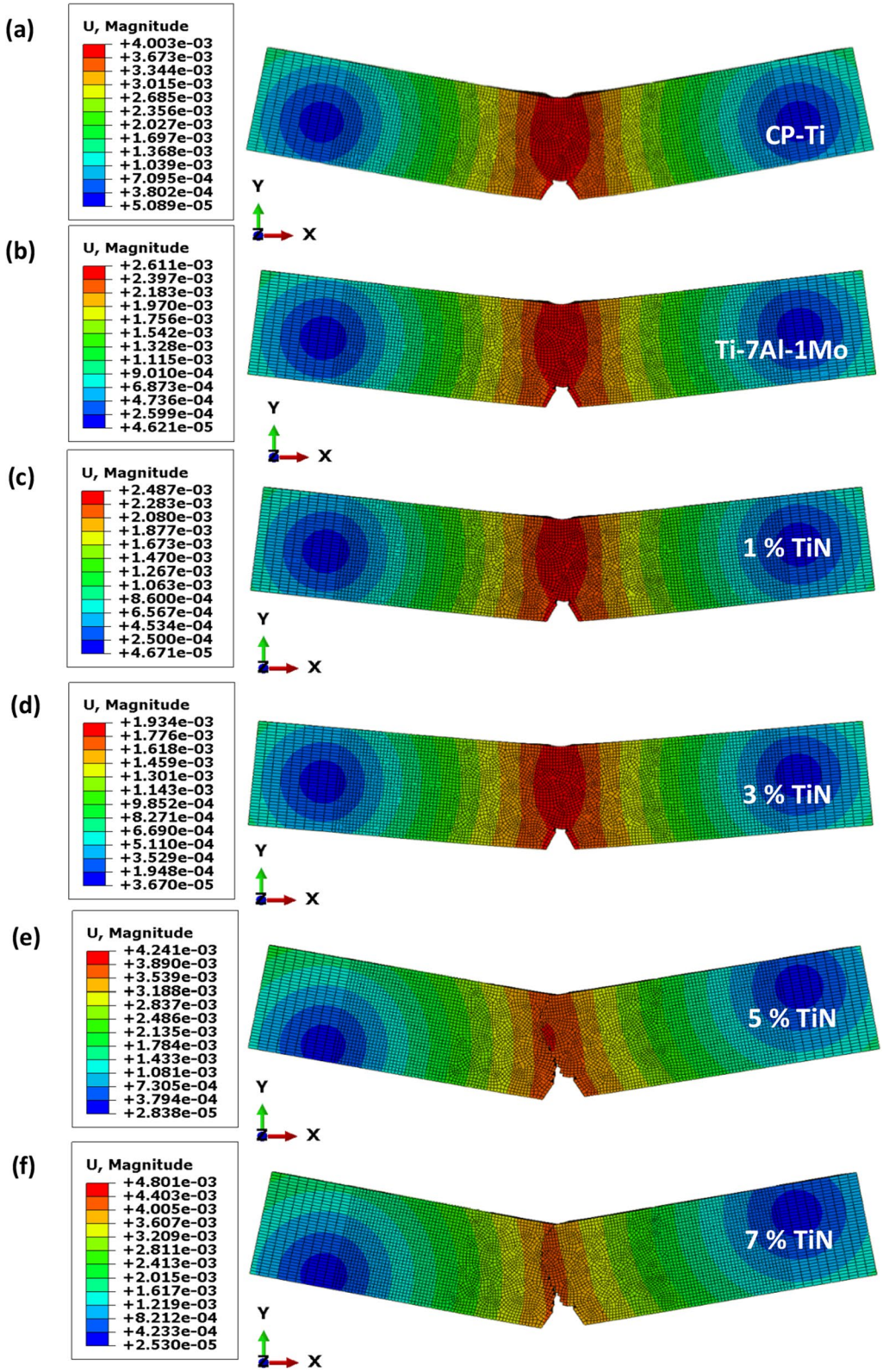

Fig. 6 Displacement magnitude within the tested models with varying wt% of TiN

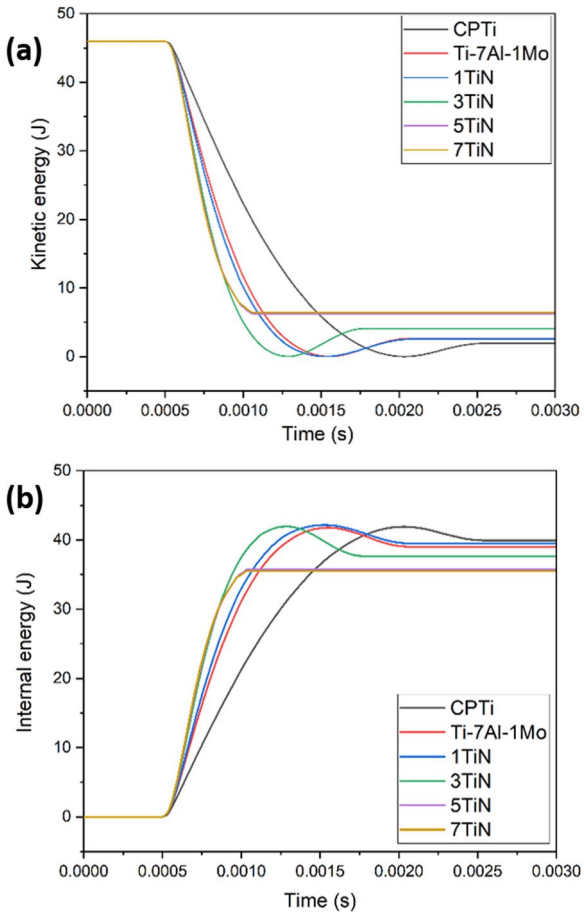

Fig. 7 **a** the kinetic energy of the impactor and **b** the internal energy of the tested models with varying wt% of TiN

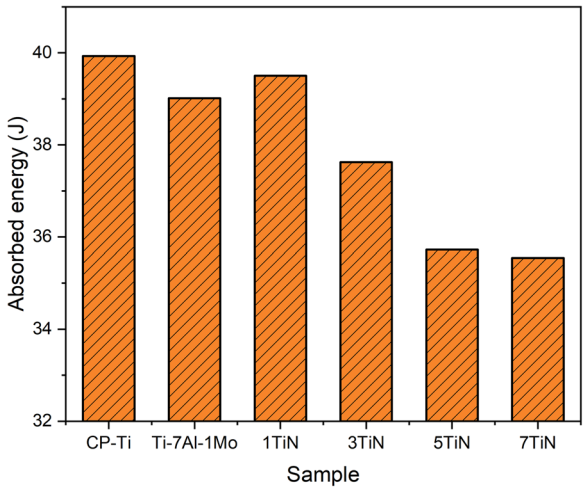

Fig. 8 Absorbed energy by the tested Models with varying wt% of TiN

kinetic energy dissipated by the impactor is nearly equal to the internal energy of the tested sample. The kinetic energy curves (Fig. 7a) show that the kinetic energy of all the samples decreases rapidly after impact.

The rate at which the kinetic energy decreases varies from sample to sample. CP-Ti has the highest kinetic energy rate, followed by Ti–Al–Mo ternary alloy, and the rate decreases as the wt% of the TiN increases. Samples with 5 wt% and 7 wt% of TiN had a more gradual decrease in kinetic energy and a more gradual increase in internal energy.

After the impact, it was observed that all samples exhibited elastic behavior, specifically in the linear portion of the curve, at approximately 0.5 ms. The duration at which this elastic behavior occurred could be utilized to elucidate the relative modulus of elasticity [19]. CP-Ti exhibits a relatively wide elastic region of approximately 1.24 ms, indicating a lower elastic modulus. In contrast, composites containing 3 wt%, 5 wt%, and 7 wt% of TiN demonstrate an extended elastic region of approximately 0.829 ms, indicating a higher elastic modulus.

According to the findings presented in Fig. 7b, it can be observed that CP-Ti, Ti–7Al–1Mo, Ti–7Al–1Mo/1TiN, and Ti–7Al–1Mo/3TiN exhibit a comparable pattern in the internal energy curve. This pattern is characterized by a parabolic peak, which suggests the occurrence of plastic deformation [20]. The width of the parabola serves as an indicator of the extent of plastic deformation [21]. The plastic deformation, also known as ductility, was found to be the greatest in commercially pure titanium (CP-Ti). This observation aligns with the displacement magnitude depicted in Fig. 6. The internal energy reached its highest value in all samples, with the exception of composites containing 5 wt% and 7 wt% of TiN. The maximum internal energy observed in these samples was approximately 42 J, which is approximately 3.975 J lower than the initial kinetic energy of the impactor. The observed phenomenon can be ascribed to the dissipation of energy through plastic deformation and frictional processes [22]. A limited amount of plastic deformation was observed in the composites containing 5 wt% and 7 wt% of TiN prior to fracture, owing to the inherent brittleness of the samples.

Figure 8 displays the graphical representation of the absorbed energy for all the models that were subjected to testing. The absorbed energy of a sample can be used to calculate the impact resistance of the material. The impact resistance is a measure of the material's ability to withstand impact damage. The higher the absorbed energy, the higher the impact resistance of the material. An inverse relationship was observed between the level of reinforcement and the amount of absorbed energy. A decrease in absorbed energy has been observed to promote the rapid transition of the failure mode from

a ductile state to a brittle state [23]. Therefore, this provides a rationale for the observed crack propagation in the composite material containing a higher weight percentage of reinforcement.

The observed trend in the decrease of absorbed energy during FEA is directly correlated with the increase in weight percentage of TiN reinforcement, up to a maximum of 3 wt%. This trend suggests that the potential trade-off between reduced toughness and improved strength/stiffness in the models is negligible.

4 Discussion

4.1 Von Mises stress distribution of tested samples

The observed rise in the maximum stress of Ti–7Al–1Mo ternary alloy as compared to CP-Ti (Fig. 5) can be attributed to the phenomenon of solid solution strengthening in aluminum, as discussed in previous studies [1, 3]. The von Mises stress is a measure of the overall stress state at a point in a material, and it is a useful quantity for predicting plastic deformation and failure; The aforementioned criterion is employed for the purpose of assessing the yield strength of a specific material [24, 25]. It is anticipated that the absorbed energy of a specific material will decrease as the yield strength increases, as a result of processes that lead to its hardening, such as alloying or reinforcement. Consequently, the material's ability to undergo significant plastic deformation is diminished [26].

All samples were found to experience a degree of plastic deformation. The absence of the characteristic 'U' shaped plastic deformation at the point of contact between the impactor and the tested sample suggests a transition toward a brittle state. In addition, the presence of shear bands in the composite reinforced with 5 wt% and 7 wt% of TiN nanoceramic suggests that they are more likely to fail by ductile fracture. This is likely due to the fact that TiN is a harder and more brittle material than Ti–Al–Mo. As a result, TiN-rich composites are less likely to deform plastically, and they are more likely to fail by brittle fracture. Hence, it can be observed that other reinforced compacts have undergone a strengthening process, resulting in an acceptable decrease in toughness.

4.2 Displacement magnitude of tested samples

The notches have been identified as areas of stress concentration [27]. Therefore, it is anticipated that the maximum displacement in the Charpy impact test will occur in the direction of the impactor's motion or the initiation of the crack from the notch. Displacement serves as a reliable metric for assessing the stiffness of a material, which refers to its capacity to resist deformation when subjected to impact [28, 29]. The enhancement experienced in composites reinforced with TiN nanocomposites suggests that the stiffness characteristics of CP-Ti and Ti–7Al–1Mo ternary alloy experienced notable enhancement despite the decrease in ductility. Given the observation that the composites containing 5 wt% and 7 wt% of TiN experienced fracture, it is evident that they exhibited the highest magnitude of maximum displacement, as anticipated.

4.3 Energy behavior of the model of tested samples

The quantification of toughness in a material can also be achieved through the measurement of impact energy [30, 31]. The experimental findings from Fig. 7 indicate that the amount of kinetic energy dissipated by the impactor is nearly equal to the internal energy of the tested sample. The rapid decrease in the kinetic energy of all the samples after impact (Fig. 7a) can be attributed to the fact the kinetic energy is converted into internal energy (deformation and heat) and other forms of energy, such as acoustic energy [32]. The interrelation among kinetic energy, internal energy, and other energy forms can be elucidated by the principle of energy conservation:

The sum of the energy of an object is equal to the energy due to its motion, the energy associated with its internal molecular activity, and any other forms of energy present. From a mathematical standpoint, this can be expressed as seen in Eq. 2.

$$E_T = K_E + U + E_{other} \tag{2}$$

where E_T is the total energy of the system; K_E is the kinetic energy of the system; U is the internal energy of the system (plus heat and deformation); and E_{other} is other forms of energy (e.g., light energy, acoustic energy).

The decreases in the rate of kinetic energy as the wt% of the TiN increases can be ascribed to the fact that samples with higher impact energies have faster rates of internal energy increase. That is the higher impact energies result in more energy being transferred to the samples, which causes them to deform more rapidly. Composites with 5 wt% and 7 wt% of TiN reinforcements had a more gradual decrease in kinetic energy and a more gradual increase experience due to ductile fracture.

The absorbed energy of a sample can be used to calculate the impact resistance of the material. The impact resistance is a measure of the material's ability to withstand impact damage. The higher the absorbed energy, the higher the impact resistance of the material. The decrease in absorbed energy observed as the level of reinforcement increases as seen in Fig. 8 promotes the rapid transition of the failure mode from a ductile state to a brittle state [23]. Therefore, this provides a rationale for the observed crack propagation in the composite material containing a higher weight percentage of reinforcement.

The observed trend in the decrease of absorbed energy during FEA is directly correlated with the increase in weight percentage of TiN reinforcement, up to a maximum of 3 wt%. This trend suggests that the potential trade-off between reduced toughness and improved strength/stiffness in the models is negligible.

5 Conclusion

The FEA approach was used to successfully model the Charpy impact behavior of CP-Ti, Ti–Al–Mo ternary alloy, and the Ti–Al–Mo/yTiN ($y = 1$, 3, 5, and 7) composites. All of the sintered compacts' von Mises stress distribution, magnitude of displacement, and energy behavior were examined.

- The study revealed a positive correlation between the level of reinforcements and the von Mises stress observed within the tested model.
- The CP-Ti and Ti–7Al–1Mo ternary alloy models exhibited the highest magnitudes of displacement without fracture. However, in the TiN-reinforced samples, these values decreased with increasing TiN weight percentage up to 3%."
- The absorbed energy exhibited a decline with an increase in the weight percentage of reinforcement.
- The models containing 5 wt% and 7 wt% of TiN nanoceramic exhibit a low level of plastic deformation prior to reaching the point of fracture.
- In general, it can be inferred that the strength and stiffness of the models were enhanced as the weight percentage of TiN reinforcement increased, up to a concentration of 3 wt% of TiN. This improvement was achieved at the expense of a tolerable decrease in toughness.

Acknowledgements
The authors acknowledge the financial support for this research by the Faculty of Engineering and Built Environment, Tshwane University of Technology, and the Department of Chemical, Metallurgical and Materials Engineering of the Tshwane University of Technology, Pretoria, South Africa.

Author contributions
This work was carried out in conjunction with all authors. The role of each author is as listed as follows: SOJ contributed to conceptualization, methodology, software, investigation, analysis, and writing—original draft preparation. TM involved in analysis and writing—review and editing. MBS involved in supervision, analysis, and writing—review and editing.

Funding
Not applicable.

Availability of data and materials
The datasets used and/or analyzed during the current study are available from the corresponding author on reasonable request.

Declarations

Ethics approval and consent to participate
Not applicable.

Consent for publication
Not applicable.

Competing interests
The authors declare no competing financial interests or personal relationships that could have appeared to influence the work reported in this paper.

Author details
[1]Department of Chemical, Metallurgical and Materials Engineering, Faculty of Engineering and Built Environment, Tshwane University of Technology, Pretoria 0001, South Africa.

Received: 13 December 2023 Accepted: 12 February 2024
Published online: 22 February 2024

References

1. Jeje SO, Shongwe MB, Maledi N, Ogunmuyiwa EN, Tshabalala LC, Babalola BJ, Olubambi PA (2020) Sintering behavior and alloying elements effects on the properties of CP-Titanium sintered using pulsed electric current. Mater Chem Phys 256:123707
2. Jeje SO, Shongwe MB, Maledi N, Rominiyi AL, Adesina OS, Olubambi PA (2021) Synthesis and characterization of TiN nanoceramic reinforced Ti–7Al–1Mo composite produced by spark plasma sintering. Mater Sci Eng A 807:140904
3. Jeje SO, Shongwe MB, Ogunmuyiwa EN, Rominiyi AL, Olubambi PA (2020) Microstructure, hardness, and wear assessment of spark-plasma-sintered Ti–x Al–1Mo alloy. Metall and Mater Trans A 51:4033–4044
4. Szutkowska M, Cygan S, Podsiadło M, Laszkiewicz-Łukasik J, Cyboroń J, Kalinka A (2019) Properties of TiC and TiN reinforced alumina–zirconia composites sintered with spark plasma technique. Metals 9(11):1220
5. Guo B, Zhou J, Zhang S, Zhou H, Pu Y, Chen J (2008) Microstructure and tribological properties of in situ synthesized TiN/Ti3Al intermetallic matrix composite coatings on titanium by laser cladding and laser nitriding. Mater Sci Eng, A 480(1–2):404–410
6. Huang S, Zhao Q, Lin C, Wu C, Zhao Y, Jia W, Mao C (2021) Effects of oxygen content on Charpy impact properties and crack resistance of α titanium alloys. Mater Sci Eng, A 818:141394
7. Alaneme KK, Kareem SA, Ozah BN, Alshahrani HA, Ajibuwa OA (2022) Application of finite element analysis for optimizing selection and design of Ti-based biometallic alloys for fractures and tissues rehabilitation: a review. J Mark Res 19:121–139
8. Zienkiewicz OC, Cheung YK (1967) The finite element in structural and continuum mechanics. Mcgraw-Mill Puolishing Company Limited 1967 年
9. Lammari L, Khlifa SB, Abdelli S, Slama C, Kharroubi H (2022) Numerical modeling of a Charpy test study of the impact resistance of low alloy steels and unalloyed steels. Res Invent: Int J Eng Sci 12(8):1–10
10. Yu H, Jeong DY, Gordon JE, Tang YH (2007) Analysis of impact energy to fracture unnotched charpy specimens made from railroad tank car steel. In: Rail transportation division conference, Vol 48000, pp 123–130
11. Jeong DY, Yu H, Gordon JE, Tang YH (2008) Finite element analysis of unnotched Charpy impact tests
12. Madhusudhan D, Chand S, Ganesh S, Saibhargavi U (2018) Modeling and simulation of Charpy impact test of maraging steel 300 using Abaqus. In: IOP conference series: materials science and engineering, IOP Publishing, Vol 330, No. 1, p 012013
13. Zhao S, Xu Y, Pan C, Liang L, Wang X (2019) Microstructural modeling and strengthening mechanism of TiB/Ti–6Al–4V discontinuously-reinforced titanium matrix composite. Materials 12(5):827
14. Cheon YJ, Kim HG (2018) An efficient contact algorithm for the interaction of material particles with finite elements. Comput Methods Appl Mech Eng 335:631–659

15. Said NM, Ali MB (2016) Analysis of impact duration from Charpy impact signal. Proc Mechan Eng Res Day 2016:161–162
16. Li J, Zhang T, Wang S, Cheng J, Wang W (2023) Mechanism and method of testing fracture toughness and impact absorbed energy of ductile metals by spherical indentation tests. Chin J Mech Eng 36(1):108
17. Abaqus GJDSSC, Providence, RI, USA, Abaqus 6.11. 2011: p 3
18. Jia W, Pi A, Zhao Z, Wang S, Wei C, Jie Z, Huang F (2022) Study on intrinsic influence law of specimen size and loading speed on Charpy impact test. Materials 15(11):3855
19. Jayadeep UB, Bobji MS, Jog CS (2014) Energy loss in the impact of elastic spheres on a rigid half-space in presence of adhesion. Tribol Lett 53:79–89
20. Meyer LW, Halle T, Abdel-Malek S (2009) Experimental and numerical investigations on the behavior of steel plates and structures under impact loading. In: DYMAT-international conference on the mechanical and physical behaviour of materials under dynamic loading, EDP Sciences, Vol 1, pp 73–79
21. Yudhanto A, Wafai H, Lubineau G, Goutham S, Mulle M, Yaldiz R, Verghese N (2019) Revealing the effects of matrix behavior on low-velocity impact response of continuous fiber-reinforced thermoplastic laminates. Compos Struct 210:239–249
22. Yasuhito T, Fumiyoshi M (2017) Influence of impact velocity on transition time for V-notched Charpy specimen. 溶接学会論文集 35(2):80–84
23. Madhusudhan D, Chand S, Ganesh S, Saibhargavi U (2018) Modeling and simulation of Charpy impact test of maraging steel 300 using Abaqus. In: IOP conference series: materials science and engineering, IOP Publishing, Vol. 330, No. 1, p 012013
24. Huang Y, Jiang J (2023) A critical review of von mises criterion for compatible deformation of polycrystalline materials. Crystals 13(2):244
25. González-Velázquez JL (2020) Mechanical behavior and fracture of engineering materials. Springer
26. Kim K, Park M, Jang J, Kim HC, Moon HS, Lim DH, Kim BJ (2018) Improvement of strength and impact toughness for cold-worked austenitic stainless steels using a surface-cracking technique. Metals 8(11):932
27. Moore PL, Booth G (2014) The welding engineer's guide to fracture and fatigue. Elsevier
28. Goodyear SR, Aspden RM (2019) Mechanical properties of bone ex vivo. Bone Res Protoc. https://doi.org/10.1007/978-1-61779-415-5_35
29. Lu SK, Hua DX, Li Y, Cui FY, Li PY (2019) Stiffness calculation method and stiffness characteristic analysis of bolted connectors. Math Probl Eng
30. Oral E (2011) Polymeric joint bearing surfaces for total joint replacements. In: Biomaterials for artificial organs, Woodhead Publishing, pp 56–80
31. Al-Maharma AY, Sendur P (2018) Review of the main factors controlling the fracture toughness and impact strength properties of natural composites. Mater Res Expr 6(2):022001
32. Chi H, Gong B (2020) Analysis of energy conversion law in vehicle collision accident. In: Journal of physics: conference series, IOP Publishing, Vol. 1486, No. 7, p. 072014

Publisher's Note